Atmos. Chem. Phys. Discuss., 12, 24043–24093, 2012
www.atmos-chem-phys-discuss.net/12/24043/2012/
doi:10.5194/acpd-12-24043-2012


Atmospheric Chemistry and Physics Discussions



# Long-term observations of aerosol size distributions in semi-clean and polluted savannah in South Africa

**V. Vakkari[1], J. P. Beukes[2], H. Laakso[1], D. Mabaso[3], J. J. Pienaar[2], M. Kulmala[1], and L. Laakso[2,4]**

[1]Department of Physics, University of Helsinki, P.O. Box 64, 00014 University of Helsinki, Finland
[2]School of Physical and Chemical Sciences, North-West University, Potchefstroom, South Africa
[3]Rustenburg Local Municipality, Rustenburg, South Africa
[4]Finnish Meteorological Institute, Research and Development, P.O. Box 503, 00101, Finland

Received: 12 June 2012 – Accepted: 3 September 2012 – Published: 14 September 2012

Correspondence to: V. Vakkari (ville.vakkari@helsinki.fi)

Published by Copernicus Publications on behalf of the European Geosciences Union.







## Abstract

This study presents a total of four years of sub-micron aerosol particle size distribution measurements in the Southern African savannah, an environment with few previous observations covering a full seasonal cycle and the size range below 100 nm. During the first 19 months, July 2006–January 2008, the measurements were carried out at Botsalano, a semi-clean location, whereas during the latter part, February 2008–May 2010, the measurements were carried out at Marikana (approximately 150 km east of Botsalano), which is a more polluted location with both pyrometallurgical industries and informal settlements nearby.

The median total concentration of aerosol particles was more than four times as high at Marikana than at Botsalano. In the size ranges of 12–840 nm, 50–840 nm and 100–840 nm the median concentrations were 1850, 1280 and 700 particles $cm^{-3}$ at Botsalano and 7800, 3800 and 1600 particles $cm^{-3}$ at Marikana, respectively.

The diurnal variation of the size distribution for Botsalano arose as a result of frequent regional new particle formation. However, for Marikana the diurnal variation was dominated by the morning and evening household burning in the informal settlements, although regional new particle formation was even more frequent than at Botsalano. The effect of the industrial emissions was not discernible in the size distribution at Marikana although it was clear in the sulphur dioxide diurnal pattern, indicating the emissions to be mostly gaseous.

Seasonal variation was strongest in the concentration of particles larger than 100 nm, which was clearly elevated at both locations during the dry season from May to September. In the absence of wet removal during the dry season the concentration of particles larger than 100 nm had a correlation above 0.7 with CO for both locations, which implies incomplete burning to be an important source of aerosol particles during the dry season. However, the sources of burning differ: at Botsalano the rise in concentration originates from regional wild fires, while at Marikana domestic heating in the informal settlements is the main source.





ACPD

12, 24043–24093, 2012



Air mass history analysis for Botsalano identified four regional scale source areas in Southern Africa and enabled the differentiation between fresh and aged rural background aerosol originating from the clean sector, i.e., western sector with very few large anthropogenic sources. Comparison to size distributions published for other comparable environments in Northern Hemisphere shows Southern African savannah to have a unique combination of sources and meteorological parameters. The observed strong link between combustion and seasonal variation is comparable only to the Amazon basin; however the lack of long-term observations in the Amazonas does not allow a quantitative comparison.

All the data presented in the figures, as well as the time series of monthly mean and median size distributions are included in numeric form as a Supplement to provide a reference point for the aerosol modelling community.

## 1 Introduction

Atmospheric aerosol particles impact our lives in several ways. They moderate climate via directly scattering and absorbing solar radiation and indirectly by modifying the properties of clouds and therefore affecting the global radiation budget (e.g. Seinfeld and Pandis, 2006). In addition to climate impacts, aerosol particles cause adverse health effects and deteriorate visibility (e.g. Charlson, 1969; Pope and Dockery, 2006). Atmospheric aerosol particles are recognised as the source of the largest uncertainty in the current global climate models (Forster et al., 2007). Reducing the uncertainty in the global climate models requires temporally and spatially representative data sets on a global scale, preferably including both chemical and physical properties of the aerosol particles. One of the key physical parameters of aerosols is the number size distribution, and especially for the climate effects, the size distribution in the sub-micron range.

Aerosol size distribution measurements covering at least one full year have been conducted in a number of locations, e.g. the data set compiled by Spracklen





ACPD
12, 24043–24093, 2012



et al. (2010) for comparison with a global aerosol model. However, most of the long-term observations are from the Northern Hemisphere and very few from continental locations in the Southern Hemisphere (Spracklen et al., 2010). Since the study by Spracklen et al. (2010) even more data sets have been published for the continental boundary layer in the Northern Hemisphere. For example Asmi et al. (2011) presented two years of size distributions from 20 European stations, Hyvärinen et al. (2011) more than two years of size distributions from two sites in India and Shen et al. (2011) more than a year of size distributions from the North China Plain.

However, for the Southern Hemisphere there is a very limited number of long-term data sets of sub-micron aerosol particle size distributions in the continental boundary layer (Laakso et al., 2006; Laakso et al., 2008; Hirsikko et al., 2012; Laakso et al., 2012). Even from the Amazon basin, where several intensive measurement campaigns have been carried out during recent years, no size distribution measurements that cover a full year have been published (see e.g. the review by Martin et al. (2010) and references therein).

The locations of currently available (published or accessible via databases) long-term data sets representing continental boundary layer are illustrated in Fig. 1. Figure 1 is based on the data set by Spracklen et al. (2010) and follows the division into marine, high altitude and continental boundary layer locations by Spracklen et al. (2010). Figure 1 was updated with this study and other recently published aerosol size distribution observations in the continental boundary layer extending below 100 nm and covering at least one full seasonal cycle (Asmi et al., 2011; Hyvärinen et al., 2011; Shen et al., 2011; Hirsikko et al., 2012; Laakso et al., 2012).

The only exception to the rule of one full seasonal cycle was made to have one comparison location in South America. The data set in South America in Fig. 1 refers to Rissler et al. (2006) who measured size distributions extending below 100 nm during the transition from dry to wet season in the South Western Amazon basin. The Rissler et al. (2006) data set was selected from the Amazon basin also because of its location in an agricultural (i.e., deforested) area comparable to savannah.





ACPD
12, 24043–24093, 2012



For Southern Africa the main source of information on atmospheric aerosol particles has been the SAFARI 2000 campaign (Swap et al., 2003). However, as SAFARI 2000 was focused on wild fires, the size distribution measurements were biased toward measuring emissions from fires. The measurements were conducted onboard of aircrafts to enable the tracking of fire plumes and hence the data sets gathered were typically only for some tens of hours of flight time (Haywood et al., 2003a,b; Hobbs et al., 2003; Ross et al., 2003). The campaign was conducted in September 2000, which is usually part of the peak period for wild fires, i.e., the late dry season. Furthermore the wild fires were exceptionally intense in September 2000 (Swap et al., 2003), if compared with an average burning season. Considering all the above, the measurements during SAFARI 2000 are therefore not temporally or spatially representative of the typical aerosol particle size distribution in Southern Africa.

Since SAFARI 2000 the next observations on sub-micron aerosol particle size distribution in Southern Africa were published by Laakso et al. (2008), who presented the monthly statistics of the number concentration of 10 to 840 nm aerosol particles measured at Botsalano from July 2006 to July 2007. Laakso et al. (2008) were the first to cover one full seasonal cycle in Southern Africa; however, the paper did not give more details than the monthly medians and percentiles of the observed total concentration. Recently Hirsikko et al. (2012) briefly discussed the diurnal and seasonal variations of the sub-micron aerosol size distribution in connection to new particle formation at Marikana village, 150 km east of Botsalano, from February 2008 to May 2010. Laakso et al. (2012) included seasonal variation of aerosol number concentration from 10 nm to 10 µm in an overview of measurements at Elandsfontein, 200 km east of Marikana, from February 2009 to January 2011, that were part of the South African component of the European Union sponsored project EUCAARI (Kulmala et al., 2009, 2011).

To partially fill the gap in the size distribution data for Southern Africa we present here nearly four years of sub-micron aerosol size distribution measurements in South Africa. The first part of the measurements was conducted in a semi-clean background location (Laakso et al., 2008) and the second in a more polluted area with mixed





ACPD
12, 24043–24093, 2012



industrial sources and some informal settlements (Hirsikko et al., 2012; Venter et al., 2012) enabling a comparison between clean and polluted size distributions. The aforementioned measurement campaigns were supported also by the EUCAARI South African component (Kulmala et al., 2009, 2011; Laakso et al., 2012).

The diurnal, seasonal and spatial variations of sub-micron aerosol size distribution were analysed and the differences between the semi-clean and the polluted environment discussed. Additionally, we have included all the data used in the figures, as well as the monthly averaged time series of the size distributions in full size resolution as a Supplement to provide a reference point for future modelling studies.

## 2 Measurements and methods

### 2.1 Location

This study presents size distributions from two locations in the North-West Province of the Republic of South Africa. The measurements were conducted in Botsalano game reserve, latitude 25.54° S, longitude 25.75° E, 1420 m a.s.l., from 20 July 2006 until 5 February 2008 (Laakso et al., 2008; Vakkari et al., 2011) and in Marikana village, latitude 25.70° S, longitude 27.48° E, 1170 m a.s.l., from 8 February 2008 to 17 May 2010 (Hirsikko et al., 2012; Venter et al., 2012).

The Botsalano game reserve has no local sources and has an extensive clean sector to the west, with very little anthropogenic activities (Laakso et al., 2008). However, the prevailing air mass origin for Botsalano is from the anticyclonic recirculation path, which accumulates emissions from the entire industrialised Highveld (Tyson et al., 1996; Vakkari et al., 2011). The median $SO_2$ concentration is therefore nearly 1 ppb at Botsalano and hence the site is described as semi-clean instead of clean background site (Laakso et al., 2008). Botsalano is also occasionally affected by direct plumes from the megacity of Johannesburg-Pretoria (Lourens et al., 2012) and the surrounding industry (Vakkari et al., 2011).





ACPD
12, 24043–24093, 2012



Marikana, on the other hand is in the middle of the pyrometallurgical industry surrounding the city of Rustenburg approximately 100 km north-west of the Johannesburg-Pretoria megacity and 150 km east of Botsalano (Hirsikko et al., 2012; Venter et al., 2012). The pyrometallurgical industry around Marikana consists mainly of platinum group metal smelters that have high $SO_2$ emissions (Venter et al., 2012) and ferrochrome smelters (Beukes et al., 2010). In addition to the industrial sources there are also informal settlements and low-cost housing in the Marikana village and the site is impacted daily by the household cooking and space heating activities in these areas (Hirsikko et al., 2012; Venter et al., 2012). Because of the significance of the industrial sources the area surrounding the measurement site at Marikana has been proposed as a third legislatively proclaimed national air pollution hotspot in South Africa (Scott, 2010), in addition to the two existing priority areas, i.e., the Vaal Triangle and the Highveld priority areas (Yako, 2005; van Schalkwyk, 2007). Wild fires are frequent during the dry season in Southern Africa and may occur in any direction from the afore-mentioned measurement sites.

Marikana is located close to the transitional zone of the grassland biome to the savannah biome (Mucina and Rutherford, 2006). The area surrounding Marikana that are not in industrial or residential use, are mainly used for farming activities, including both grazing and cash crop (e.g. maize) production (Venter et al., 2012). The Botsalano game reserve is situated totally in the savannah biome, which also supports agricultural use (Friedl et al., 2002; Laakso et al., 2008). The clean sector west of Botsalano changes within approximately 100 km into semi-arid shrublands with low biomass and biological activity (Friedl et al., 2002; Mucina and Rutherford, 2006). This biome continues in the sector between north and west from Botsalano into the neighbouring countries of Botswana and Namibia. This region is commonly referred to as the Kalahari. To the south-west of Botsalano the mixed grassland/savannah vegetation changes within a couple of hundred kilometres into the dry Karoo biome, which has even less biomass and biological activity than the Kalahari.





ACPD
12, 24043–24093, 2012



## 2.2 Instrumentation

The measurements were carried out at both Botsalano and Marikana with a mobile measurement trailer, which has been described in detail by Petäjä et al. (2007) and Laakso et al. (2008). In this study we utilise only the aerosol particle size distributions from the differential mobility particle sizer (DMPS) (Hoppel, 1978; Jokinen and Mäkelä, 1997), size range 12–840 nm, time resolution 10 min, and as auxiliary data the CO and $SO_2$ concentrations measured with Horiba APMA-360 and Thermo 42S analysers, respectively.

Data coverage of the aerosol particle size distribution measurements from the DMPS was 75 % for the entire measurement period combined at both sites. For Botsalano problems at the beginning of the measurement campaign, i.e., irregularities in the incoming power and CPC breakdown in September 2006, decreased the average data coverage to 69 %. However from January 2007 onwards until the end of the measurements at Botsalano on 5 February 2008 the data coverage was on average 82 %.

For Marikana the average data coverage was 80 %. From the start of the measurements on 10 February 2008 until the end of July 2009 the data coverage was good, on average 90 %, but during the second half of the Marikana measurement campaign some technical problems occurred: a CPC breakdown at the end of July 2009, a virus infection in the measurement PC in December 2009–January 2010 and a leak in the DMPS sheath air pump in March–April 2010. Nevertheless, the monthly data coverage for both campaigns presented in Fig. 2 shows that the gaps in the measurements do not hinder studying seasonal variation.

A TSI 3772 CPC was running in parallel with the trailer DMPS for one week in August 2011. While the concentration was below 10 000 particles $cm^{-3}$, i.e., the 3772 CPC operating in single particle count mode, the DMPS total concentration was on average (median) 2 % higher than the TSI 3772 concentration. The 25th and 75th percentiles of the ratio of the DMPS to the TSI 3772 concentration were 0.97 and 1.10, respectively, which are comparable to the counting accuracy of a CPC.





ACPD
12, 24043–24093, 2012



### 2.3 Size distribution parameters

Number concentrations of aerosol particles larger than 50 or 100 nm in diameter are quite commonly used as proxies of cloud condensation nuclei (CCN), when direct measurements of CCN do not exist (e.g. Asmi et al., 2011). In this study, these number concentrations are approximated by integrating the measured size distribution concentrations from 50 to 840 nm ($N50$) and from 100 to 840 nm ($N100$) in particles $cm^{-3}$. To provide a more comprehensive overview of the data, the size distribution number concentrations are also integrated from 12 to 840 nm ($N12$) and from 12 to 25 nm ($N < 25$) ($cm^{-3}$) and, in addition to the sectional number concentrations, log-normal size distribution fits also are calculated.

The fitting of the log-normal size distribution to the measured aerosol particle size distribution was done with the method described by Vartiainen et al. (2007). An $n$-modal log-normal size distribution is here defined with 10-base logarithm as

$$\frac{dN}{d\log_{10}(D_p)} = \sum_{i=1}^{n} \frac{N_i}{\sqrt{2\pi}\log_{10}(\sigma_i)} \exp\left(-\frac{\left(\log_{10}(D_p) - \log_{10}(\mu_i)\right)^2}{2\left(\log_{10}(\sigma_i)\right)^2}\right) \quad (1)$$

where $D_p$ is the particle diameter in nm, $N_i$ is particle number in mode $i$, $\mu_i$ is the geometric mean of the mode $i$ in nm and $\sigma_i$ is the standard deviation of mode $i$ (Seinfeld and Pandis, 2006). In this method (Vartiainen et al., 2007) the number of modes per size distribution, n, is allowed to vary freely from one to three to obtain the best fit. Also the geometric means of the modes ($\mu_i$) are left unconstrained.

While the modal fits presented in this study describe the size distribution in more detail than the number concentrations of $N12$, $N < 25$, $N50$ and $N100$, it is also a potential source of error. The error of the modal fits is estimated as the mean relative error of the fitted size distribution in percent, MRE. MRE is calculated as the arithmetic mean of the relative error of the fitted distribution $n_{fit}$ compared to the measured size





ACPD
12, 24043–24093, 2012



distribution $n_{obs}$

$$\mathrm{RME} = \frac{\sum_{i=i_1}^{i_2} \frac{n_{obs}(D_p(i)) - n_{fit}(D_p(i))}{n_{obs}(D_p(i))}}{(i_2 - i_1 + 1)} \times 100\,\% \quad (2)$$

where $D_p$ is the size resolution vector of the measured distribution $n_{obs}$ as $\frac{dN}{d\log_{10} D_p}$ and the limits of the summation $i_1$ and $i_2$ can be selected to cover the entire range of the size distribution or only a fraction of it. The $n_{fit}$ here is calculated from Eq. (1).

Especially at the larger particle sizes the size distribution was quite often not log-normal for both Botsalano and Marikana, which led to over- or underestimation of the size distribution by the modal fits. To account for this, we have calculated the MRE separately for the distribution both below and above 300 nm in addition to the overall error.

For the Botsalano median distribution, Fig. 3, the modal fits represented the distribution quite well below 300 nm with a mean relative error of 5 %, but above 300 nm the fits overestimated the concentration by on average 30 %. For Marikana the modal fits were closer to the median distribution with a 0.5 % mean relative error below 300 nm and 8 % mean relative error above 300 nm.

Since the concentrations above 300 nm were not large, even a 30 % overestimate of the size distribution did not affect the total concentration significantly. For example for the Botsalano median distribution using the log-normal modal fits instead of the measured data to calculate $N100$ led to an error of 0.9 %. However, we recommend using the primary data instead of the modal fits whenever possible.

The number size distributions are presented as $\frac{dN}{d\log_{10} D_p}$ with units of particles $\mathrm{cm}^{-3}$ throughout this paper in prevailing conditions, but we have included in the Supplement the atmospheric pressure measured at the sites and the temperature of the DMPS system to facilitate comparison with concentrations given in STP conditions.





ACPD
12, 24043–24093, 2012



## 2.4 Ancillary data

The spatial variability of the size distributions was studied with air mass history from back-trajectories similarly to Vakkari et al. (2011). The 96-h back-trajectories for each hour throughout the measurement period were calculated with the HYSPLIT 4.8 model (Draxler and Hess, 2004). The HYSPLIT model was run with the GDAS meteorological archive produced by the US National Weather Service's National Centre for Environmental Prediction (NCEP) and archived by the National Oceanic and Atmospheric Administration (NOAA) Air Resources Laboratory (ARL) (Air Resources Laboratory, 2011).

In the simple approach used by Vakkari et al. (2011) a $0.5^{\circ} \times 0.5^{\circ}$ grid is first defined over Southern Africa. Each back-trajectory is then assigned the parameters observed at the measurement site when the trajectory arrived – in this case the $N12$, $N50$ and $N100$ number concentrations. Each grid cell is then allocated an average value of the observed parameters assigned to the trajectories passing over it, i.e., the value of each grid cell represents the average value observed at the measurement site when air masses passed over that point.

The accuracy of trajectories depends on the quality of the underlying meteorological data in use (Stohl, 1998) and the errors accompanying single trajectories are currently estimated as 15 to 30 % of the trajectory distance travelled (Stohl, 1998; Riddle et al., 2006). However, Vakkari et al. (2011) demonstrated that the afore-mentioned approach gives a fairly representative picture of the regional patterns around Botsalano.

The seasonality of wild fires in Southern Africa was studied using MODIS collection 5 Burned Area product (Roy et al., 2008). The MODIS Burned Area product provides an estimate of when a specific 500 m × 500 m land area has been burned based on rapid changes in the surface reflectance (Roy et al., 2008). The monthly number of fire observations at a 500 km radius around each measurement location was calculated for the entire measurement period.





ACPD
12, 24043–24093, 2012



## 3 Results and discussion

### 3.1 Median size distributions

The individual overall median distributions for both Botsalano and Marikana with modal fits are presented in Fig. 3. The median total concentration from 12 to 840 nm ($N12$) was 1800 and 7800 particles $cm^{-3}$ for Botsalano and Marikana, respectively. The median and mean number concentrations for both Botsalano and Marikana in all four size ranges ($N12$, $N < 25$, $N50$ and $N100$) are given in Table 1 together with the six reference data sets indicated in Fig. 1. Also two data sets from Southern Africa covering a full seasonal cycle are included in Table 1, although they did not present size resolved concentrations. Log-normal size distribution parameters fitted to both median and mean size distributions are presented in Table 2 for both Botsalano and Marikana.

The fitted Aitken mode concentration of Marikana (Table 2) is over four times higher than for Botsalano, although the fitted accumulation mode number concentrations are quite close to each other. Also the nucleation mode concentration is relatively high for Marikana, whereas the Botsalano median distribution below 25 nm is fairly well represented as the tail of the Aitken mode. This indicates that the measurements at Marikana were much closer to the sources of the aerosol particles than at Botsalano.

Four of the sites chosen for the comparison in Table 1, i.e., Mukteshwahr, India (Hyvärinen et al., 2011), Shangdianzi, China (Shen et al., 2011), Southern Great Plains, US (Sheridan et al., 2001) and K-Puszta, Hungary (Asmi et al., 2011), are surrounded by grassland or cropland with no local sources, although none of them are really remote locations. Mukteswahr lies approximately 200 km from the megacity of New Delhi (Hyvärinen et al., 2011) and Shangdianzi approximately 150 km from the megacity of Beijing (Shen et al., 2011). The nearest coal-fired power plants lie within 50 km of the Southern Great Plains site (Rissman et al., 2006) and K-Puszta is located only 80 km from Budapest with 1.5 million inhabitants (Asmi et al., 2011). The fifth site characterised as crop- or grassland in Table 1 is located at Fazenda Nossa Senhora Aparecida in Rondonia, Brazil approximately 50 km from the closest city of Ji-Parana





ACPD
12, 24043–24093, 2012



with 100 000 inhabitants (Rissler et al., 2006). The Rondonia site is impacted by extensive biomass burning during the dry season (Rissler et al., 2006) and thus the concentrations in Rondonia are clearly higher than in natural environment in Amazon basin (Martin et al., 2010).

The Gual Pahari site in India was included for comparison with Marikana, because both are affected by biomass burning for household heating and cooking (Hyvärinen et al., 2011; Hirsikko et al., 2012). However, Gual Pahari is only 25 km from New Delhi, thus it is impacted by the megacity (Hyvärinen et al., 2011). The Ispra site in Italy was selected to represent a more industrially polluted location (Asmi et al., 2011).

The total concentration at Botsalano is slightly lower or comparable to the other semi-clean grass- or cropland sites in Table 1, except for the Shangdianzi site (Shen et al., 2011) and the Rondonia site during the dry season (Rissler et al., 2006), which have total concentrations comparable to Marikana. However, the concentration of particles larger than 100 nm is clearly lower at Botsalano than at the other semi-clean sites except for the Southern Great Plains (Sheridan et al., 2001). One plausible explanation is that the prevailing anticyclonic recirculation of air masses for Botsalano (Vakkari et al., 2011) forces air masses from the industrial sources around Johannesburg to travel considerably longer than the direct distance to Botsalano. Longer transportation allows more time for removal processes and dilution. On the other hand the concentration below 100 nm and therefore also the total concentration are kept relatively high by the extremely high frequency of new particle formation observed at Botsalano (Vakkari et al., 2011).

The concentrations at Marikana are only slightly higher than at Shangdianzi and clearly lower than at Gual Pahari, but higher than for Ispra (Table 1). The concentration above 100 nm is lower than in any of these three sites. It seems that for Marikana the total concentration is largely due to the new particle formation, which occurs with record-high frequency (Hirsikko et al., 2012).

The two comparison datasets from Southern Africa in Table 1, Elandsfontein (Laakso et al., 2012) and Gaborone (Jayaratne and Verma, 2001), lie between the observed





ACPD
12, 24043–24093, 2012



concentrations in Botsalano and Marikana, which is reasonable considering the anthropogenic sources in the locations.

### 3.2 Diurnal variation of the size distribution

Figure 4 illustrates the median diurnal variation of aerosol particle size distribution for Botsalano and Marikana. Both surface plots have been calculated from the measurements so that each 10 min size distribution is a median for that specific time interval over the entire measurement period for each location. The edges of the new particle formation event in Fig. 4 left panel (Botsalano) are not as sharp as in a typical event, since the onset of the new particle formation follows sunrise, which varies from 05:18 to 07:01 local time (LT) at Botsalano. This time dependant variation, as well as the shape of the typical event can be seen in Appendix A Fig. A1, where median diurnal variation for Botsalano is plotted for each month.

For Botsalano new particle formation is the main driving force of the diurnal variation in the size distribution. Furthermore, the accumulation mode concentration does not appear to drop at the onset of the event, if the median diurnal behaviour or data from March to November is considered. However, during summer, i.e., December to February, there is a drop in the accumulation mode in the morning, as seen in monthly median diurnal plots in Fig. A1 in Appendix A – for mean diurnal variation the drop is stronger.

Considering the median diurnal distribution, the accumulation mode concentration increased at the onset of the new particle formation event: the increase in $N100$ in Fig. 4 is concurrent with the appearance of the nucleation mode. Even in the one hour median size distribution parameters in Table 3 the $N100$ increased from 06:00 to 12:00 LT. This is due to the growth of the pre-existing Aitken mode particles, as is seen in the modal fits of the median diurnal distribution in Fig. 5. The growth of the pre-existing Aitken mode therefore seems to be an important process producing CCN-sized particles in a semi-clean savannah environment such as Botsalano.





ACPD
12, 24043–24093, 2012



For Marikana the size distribution also presents a strong regional new particle formation event in the midday (Fig. 4). However, in addition to this the aerosol particle concentration also increased in the early morning at sunrise (after 6 o'clock local time) and again in the evening at sunset (after 18 o'clock local time). The morning and evening peaks originate from domestic space heating and cooking in the surrounding informal and semi-formal settlements (Venter et al., 2012; Hirsikko et al., 2012), which is seen also in the rise in CO concentration during corresponding time periods in Fig. 6.

The seasonal variation of sunrise and sunset times affects the Marikana median diurnal variation (Fig. 4) similarly as discussed previously for Botsalano. The dependency on sunrise and sunset in Marikana is clearly seen in Fig. A2 in Appendix A, where diurnal variation is plotted separately for each month.

The effect of the pyrometallurgical industry around Marikana is seen as a steep rise in the $SO_2$ concentration after sunrise (Fig. 6). The peak in $SO_2$ concentration at Marikana does not reflect a change in the emissions, as the industrial processes are continuous, but can rather be attributed to the development of the boundary layer (Venter et al., 2012). As the top of the boundary layer reaches the effective stack height, the $SO_2$ emissions from the stacks reach the ground level and at the same time the mixing volume of the emissions is at its minimum, which leads to a peak in the ground level concentration (Venter et al., 2012). If Fig. 4 and 6 are compared, it seems that the emissions from the industry are mainly gaseous since there is no simultaneous increase in the concentrations of $N50$ and $N100$. The onset of the regional new particle formation event does occur at the same time as the increase in the $SO_2$ concentration; however, the calculated sulphuric acid proxy cannot explain the observed growth at Marikana (Hirsikko et al., 2012).

In addition to the regional new particle formation during daytime the nucleation mode is also present during night-time at Marikana, as seen in the fitted log-normal distribution parameters in Fig. 7. The night-time nucleation mode originates from the evening household combustion peak, although most of these emissions are in Aitken mode. Figure 7 also shows that the growth of pre-existing Aitken mode particles during the





ACPD
12, 24043–24093, 2012



new particle formation event may contribute significantly to the concentration of CCN-sized particles at Marikana.

The morning and evening peaks at Marikana do however not necessarily give a regionally representative picture of the size distribution for the entire mining and metallurgical industrial region around Marikana, known as the western Igneous Bushveld Complex (Venter et al., 2012; Hirsikko et al., 2012). This is because the nights in Marikana are calm and therefore the emissions from the household combustion accumulate close to the surface, which is seen also as dilution of the concentration after sunrise in Figs. 4, 6 and 7. Even though the early morning and evening peaks might not represent the regional aerosol, they characterise the emissions from informal settlements that have not received much attention (Hirsikko et al., 2012), notwithstanding that such informal settlements are common around the cities in South Africa (Venter et al., 2012).

Of the previously published data sets selected for comparison in Table 1, diurnal variation is dominated by new particle formation all year round only in the Shangdianzi site in China (Shen et al., 2011). Also the Southern Great Plains site has higher total concentration during midday and Sheridan et al. (2001) speculate this to be due to new particle formation. However, there is no size-resolved size distribution information available for the Southern Great Plains below 100 nm and therefore the source of the diurnal variation remains unknown (Sheridan et al., 2001). In Gual Pahari, India, the morning peak from traffic and the evening peak from heating and cooking dominate the diurnal variation, although new particle formation is also seen as an increase in the total concentration during pre-monsoon and monsoon seasons (Hyvärinen et al., 2009; Raatikainen et al., 2011).

The morning and evening peaks of the Gual Pahari size distribution diurnal variation are relatively similar to the Marikana diurnal variation, but the origin and timing of the morning peak are different (Raatikainen et al., 2011). Also in Mukteswahr, India, the evening concentrations are elevated before and after the Monsoon season (Hyvärinen et al., 2009), but at that site the diurnal variation seems to depend mainly on the boundary layer evolution rather than changes in the sources (Raatikainen et al., 2011). The





ACPD
12, 24043–24093, 2012



diurnal variation in Rondonia, Brazil has a resemblance to the Marikana diurnal variation in that the highest concentrations from biomass burning are had during evening and night-time, however, there is no or little new particle formation during daytime in Rondonia (Rissler et al., 2006). The best resemblance to the Marikana morning and evening peaks has been reported by Jayaratne and Verma (2001) from Gaborone, Botswana, although their measurements only covered the size range above 100 nm. Jayaratne and Verma (2001) also interpreted the increase in evening concentration to originate in biomass burning for space heating.

### 3.3 Seasonal variation of the size distribution

The seasonality in the size distribution for both sites is strongest for the $N100$ concentration, i.e., the accumulation mode. For Marikana $N50$ also exhibit seasonal variation in addition to the underlying $N100$ seasonality. Comparing Fig. 8 and 9 shows how the highest $N50$ and $N100$ concentrations are concurrent with the highest CO concentrations.

Studying the correlation coefficient of hourly mean CO and $N100$ for each month (Fig. 10) indicates how the months with higher $N100$ concentration also have a higher correlation between CO and $N100$, which implies that the seasonal variability of the size distribution is closely associated with incomplete burning for both Botsalano and Marikana. During the dry season, from May to September, $N100$ and CO are continuously relatively highly correlated with correlation coefficient above 0.7 for both locations.

The monthly average number of MODIS Burned Area product (Roy et al., 2008) fire observations within 500 km radius of each measurement location shown in Fig. 10 indicates that for Botsalano the highest $N100$ concentrations (Fig. 8) are reached at the peak of wild fire occurrence, i.e., September. In contrast, for Marikana the highest $N100$ and $N50$ concentrations were observed already in July, which is the coldest month of the year (Fig. 10). Therefore it seems that the seasonality of $N100$ and $N50$ for Marikana during the cold winter months is determined rather by domestic space heating than regional wild fires. Additionally the seasonal peak in wild fires results in





ACPD
12, 24043–24093, 2012



continued high correlation of CO and $N100$, even after the diminishing need for domestic space heating in September. Even if only daytime data is selected for Marikana, the shape of the correlation with CO and $N100$ and the $N100$ seasonal variation stay unchanged; only the correlation with CO and $N100$ during the wet season (from October until April) is lower. The daytime $N50$ and $N12$ indicate the seasonality of the formation and growth rates (Hirsikko et al., 2012), which is reflected as increased concentrations during the wet season. However, the dry season peak in $N50$ and $N100$ still stays in July, which indicates that the household space heating and cooking remain a stronger source of particles than regional wild fires at Marikana even considering only daytime data.

The impact of burning, as wild fires and/or household combustion, alone cannot fully explain the relatively increase in the concentrations during the dry season. The absence of wet removal, combined with lower formation and growth rates during the dry season (Vakkari et al., 2011; Hirsikko et al., 2012) increases the relative importance of the afore-mentioned combustion source of aerosol particles during the dry season. This is seen as a drop in the $N100$ and CO correlation at the beginning of the wet season (Fig. 10), which usually start after middle October.

Wild fires and agricultural biomass burning have been recognised as a major source of aerosol particles during the dry season also in the Amazon basin (Martin et al., 2010). However, there are no size distribution measurements covering the complete seasonal cycle in the Amazon basin and therefore the full effect of the fires cannot be quantified (Martin et al., 2010). Rissler et al. (2006) reported the total aerosol concentration in Rondonia to be on average five times as high at the end of the dry season as during the early wet season. However, the measurements in Rondonia were conducted in an area with very intensive biomass burning, and therefore the results cannot be considered representative of more pristine regions in the Amazon Basin although they are affected by the fires as well (Rissler et al., 2006; Martin et al., 2010).

Also the Asian Brown Cloud has been shown to originate largely in biomass burning (e.g. Gustafsson et al., 2009), but in Gual Pahari and Mukteswahr the seasonality





ACPD
12, 24043–24093, 2012



seems to be due to the monsoon seasonality rather than changes in the sources (Hyvärinen et al., 2011; Raatikainen et al., 2011). Of the other measurement sites listed in Table 1 higher concentrations were reported during winter in Gaborone (Jayaratne and Verma, 2001) and Ispra (Asmi et al., 2011). However, the origin of the seasonality for Ispra is not discussed by Asmi et al. (2011) and therefore the only comparison locations where seasonality has previously been attributed to biomass burning are Rondonia (Rissler et al., 2006) and Gaborone, where the burning seems to originate in space heating (Jayaratne and Verma, 2001). In Shangdianzi the seasonality is driven by new particle formation leading to highest concentrations in spring (Shen et al., 2011) and for the Southern Great Plains the highest concentrations of particles larger than 100 nm are had during late summer, which has been attributed to windblown dust (Sheridan et al., 2001).

Therefore, barring the limited spatial coverage of the comparison data, outside of Southern Africa combustion seems to be the most important source of seasonal variation in the size distribution only in the Amazon basin, although there are no long-term data sets from the Amazon to quantify the effect over the complete seasonal cycle (Rissler et al., 2006; Martin et al., 2010). The seasonal median size distribution parameters for both Botsalano and Marikana are collated in Table 4. Here summer is defined as December to February, autumn as March to May, winter as June to August and spring as September to November.

### 3.4 Spatial variation of the size distribution

Spatial variability of the size distributions was studied by combining the size distribution measurements with back-trajectories as by Vakkari et al. (2011). However, for Marikana anthropogenic sources in the surrounding 60 km long and 30 km wide valley are so strong that they dominate the air mass history and therefore only the data from Botsalano could be used for this purpose.

Figure 11 illustrates how at Botsalano the clean, semi-arid western sector supports clearly lower particle concentrations than the eastern sector with higher biological and





ACPD
12, 24043–24093, 2012



anthropogenic activity. The source areas $N12$, $N50$ and $N100$ at Botsalano can be divided further into four regions, as indicated in Fig. 11. The first two are the clean sector west of Botsalano, which is divided into two sub-regions, i.e., the Karoo region southwest of Botsalano and the Kalahari region northwest of Botsalano. The third is the industrial hub of South Africa located around the Johannesburg-Pretoria megacity and the fourth is the anticyclonic re-circulation path (Tyson et al., 1996; Vakkari et al., 2011) that encircles the industrial hub of South Africa.

In order to obtain a more detailed picture of the size distribution within the source regions, back-trajectories were used to select a subset of the measurements best representing each source region. For the selection the time spent over each source region in Fig. 11 was first calculated for each back-trajectory. The calculated times were then linearly interpolated to the DMPS time stamps, thus attributing to each size distribution a time the air mass had spend over each of the source regions. In this manner, each 10 min size distribution could be classified according to the criteria listed in Table 5, which resulted in a total of 17 000 10 min size distributions with well-defined source region origins. The criteria in Table 5 were set to select the air masses best representing each source region, while simultaneously minimizing the contribution from other source regions.

The median distributions for the four source regions are shown in Fig. 12, which confirms the differences between the regions defined in Fig. 11. In the clean sector the Karoo size distribution is dominated by nucleation mode and in the Kalahari by accumulation mode. This can be explained by the different origin of air masses from the Karoo and the Kalahari source regions. The air masses from the Karoo source region frequently originate over the ocean, especially during times of arriving cold fronts sweeping over Southern Africa from the south-west. In contrast the Kalahari source region air masses originate over land for all of the four day back-trajectory calculations done. In addition the Karoo source region air masses have to pass over the coastal mountains reaching up to 2000 m a.s.l., which is likely to lead to increased wet removal





ACPD
12, 24043–24093, 2012



of the aerosol. Therefore the Kalahari source region can be considered as an aged clean sector and the Karoo source region as a fresh clean sector for Botsalano.

To the east of Botsalano both the re-circulation and the industrial hub source regions have high $N50$ and $N100$ concentrations compared to the clean source regions. The industrial hub differs from the re-circulation by having a higher Aitken mode concentration and slightly lower $N100$ concentration, as is seen in Table 6. This indicates that the industrial hub aerosol is fresher than the re-circulation aerosol, which is reasonable since it contains most of the large point sources, e.g. at least 13 coal fired power station without de-$SO_x$ and de-$NO_x$, several petrochemical plants, at least 13 pyrometallurgical smelters and the mega-city of Johannesburg-Pretoria, with more than 10 million inhabitants (Lourens et al., 2012). There are some individual large anthropogenic point sources also in the re-circulation source region, including one coal-fired power plant approximately 300 km northeast of Botsalano and the city of Gaborone 50 km north of Botsalano. However, there are certainly far less large anthropogenic point sources in the recirculation source region and they are also less concentrated in terms of geographical distribution.

Notwithstanding the relatively high total number concentration of the industrial hub source region, its concentration is more than three times lower than the measured concentration in Marikana, cf. Tables 1 and 2. At Marikana also the mean diameter is clearly lower than for the industrial hub source region at Botsalano, as seen in Fig. 12. This demonstrates how after 200 km of transport over relatively clean area the industrial hub source region does not represent the size distribution at the sources.

While the differences in the anthropogenic activities are clear between the western and eastern source regions, the difference in the aerosol size distribution is partly of natural origin as well. The re-circulation and industrial hub source regions lie in the savannah and grassland biomes while the Karoo and Kalahari source regions are mostly semi-arid regions, with limited coverage of the grassland biome. Vakkari et al. (2011) concluded that the amount of biological activity in the western and eastern sectors has an effect in the growth rates of aerosol particles in regional new particle formation,





ACPD
12, 24043–24093, 2012



which cannot be distinguished from anthropogenic sources in this analysis. Considering the median distributions in Fig. 12 differences observed in the median diurnal variation for the defined source regions in Fig. 13 are not surprising. The re-circulation and industrial hub source regions have distinct new particle formation events at midday. The main difference is that the industrial hub source region's new mode concentration is higher than the re-circulation source region.

The Kalahari is the only source region that does not exhibit regional new particle formation in the median diurnal variation. This is probably due to smaller concentrations of both biogenic and anthropogenic precursors if compared to the re-circulation and industrial hub source regions, because the condensation sink in Kalahari is lower than that of the eastern source regions (Vakkari et al., 2011). In the Karoo source region the combination of an even lower condensation sink than in the Kalahari source region to low growth rates (Vakkari et al., 2011) results in the nucleation mode being continuously present.

## 4 Conclusions

We have presented here a total of four years of submicron aerosol particle size distribution measurements from semi-clean and polluted Southern African savannah. Very few previous observations, extending below 100 nm and covering a full seasonal cycle, exist for this region. The median total concentration from 12 to 840 nm in the semi-clean Botsalano was 1850 particles $cm^{-3}$. In the more polluted Marikana the total concentration was more than four times higher, median 7800 particles $cm^{-3}$. The difference between the semi-clean and polluted median distributions was largest in the nucleation mode, partly because the nucleation mode was present for Marikana also at night-time.

Regional new particle formation frequency for both Botsalano and Marikana is the highest ever recorded (Vakkari et al., 2011; Hirsikko et al., 2012) and at Botsalano the diurnal behaviour of the size distribution is dominated by the new particle formation. In Marikana, however, the effect of regional new particle formation is dominated by





ACPD
12, 24043–24093, 2012



the effect of the heating and cooking in the informal and semi-formal settlements. Surprisingly the industry in Marikana does not have discernible direct effects on the size distribution, although the $SO_2$ shows clearly the emissions from the industry.

The seasonal variation of the size distribution is driven by emissions from incomplete combustion at both Botsalano and Marikana. At Botsalano the source of the combustion is the regional wild fires and the highest concentrations of $N100$ are in September, i.e., the end of the dry season and the peak of wild fire occurrence. In Marikana, however, the seasonal variation in $N100$ and $N50$ originates from the domestic heating and cooking practises in the informal and semi-formal residential areas. Consequently the highest concentrations occur in July, which is the coldest month of the year. In both locations the $N100$ and CO are correlated throughout the dry season from May to September.

Comparison of the data presented here to previously published long-term aerosol particle size distribution measurements carried out in comparable environments shows that Botsalano and Marikana have unique combinations of aerosol particle sources and meteorological conditions. Especially the strong seasonal dependency on incomplete burning differentiates the semi-clean and polluted savannah from the previous observations. The Amazon basin seems to be the only location outside Southern Africa where seasonality of the aerosol particle size distribution is dominated by wild fires and biomass burning, but the lack of measurements covering a full seasonal cycle does not allow quantifying the effect of the combustion in the Amazon basin (Martin et al., 2010).

The air mass history study revealed four different source regions for size distributions for Botsalano. For Marikana the large local sources made it impossible to distinguish source regions from the air mass history. Two of the source regions for Botsalano lie in the clean western sector: the north-western Kalahari region and the South-Western Karoo region. Because of the different meteorological patterns transporting air from the Karoo and the Kalahari to Botsalano these two clean sector source regions differ substantially. The Karoo represents fresh clean background air with very low accumulation mode concentration and a continuously present nucleation mode. The Kalahari, on the





ACPD
12, 24043–24093, 2012



other hand, represents aged clean background air and is dominated by the accumulation mode and a nearly complete absence of the nucleation mode. The concentrations from the Kalahari are lower than from the eastern sector.

In the eastern sector from Botsalano the difference between the re-circulation and the industrial hub source regions is that the industrial hub has higher concentration in Aitken mode, a sign of fresh aerosol. The $N100$ concentration from the eastern source regions is at least twice as high as the $N100$ in the western source regions and compared to the fresh clean air from the Karoo source region up to four times as high. However, the difference between the clean and polluted source regions is not only anthropogenic, but partly also natural as the eastern sector has higher biological activity and therefore higher aerosol particle formation and growth rates (Vakkari et al., 2011).

## Appendix A

Seasonal variation of the aerosol size distribution diurnal variation is presented in Fig. A1 for Botsalano and in Fig. A2 for Marikana.

**Supplementary material related to this article is available online at: http://www.atmos-chem-phys-discuss.net/12/24043/2012/acpd-12-24043-2012-supplement.zip.**

*Acknowledgements.* The authors acknowledge the financial support by the Academy of Finland under the projects Air pollution in Southern Africa (APSA) (project number 117505) and Atmospheric monitoring capacity building in Southern Africa (project number 132640) and by the European Commission 6th Framework program project EUCAARI, contract no 036833-2 (EUCAARI). The support of Rustenburg local municipality is gratefully acknowledged. The authors thank Head of Botsalano game reserve, M. Khukhela and the game reserve employees for their kind and invaluable help during our measurements.





ACPD
12, 24043–24093, 2012



## References


Air Resources Laboratory, Gridded Meteorological Data Archives, available at: http://www.arl.noaa.gov/archives.php, last access: 9 August 2011.

Asmi, A., Wiedensohler, A., Laj, P., Fjaeraa, A.-M., Sellegri, K., Birmili, W., Weingartner, E., Baltensperger, U., Zdimal, V., Zikova, N., Putaud, J.-P., Marinoni, A., Tunved, P., Hansson, H.-C., Fiebig, M., Kivekäs, N., Lihavainen, H., Asmi, E., Ulevicius, V., Aalto, P. P., Swietlicki, E., Kristensson, A., Mihalopoulos, N., Kalivitis, N., Kalapov, I., Kiss, G., de Leeuw, G., Henzing, B., Harrison, R. M., Beddows, D., O'Dowd, C., Jennings, S. G., Flentje, H., Weinhold, K., Meinhardt, F., Ries, L., and Kulmala, M.: Number size distributions and seasonality of submicron particles in Europe 2008–2009, Atmos. Chem. Phys., 11, 5505–5538, doi:10.5194/acp-11-5505-2011, 2011.

Beukes, J. P., Dawson, N. F. and Van Zyl, P. G.: Theoretical and practical aspects of Cr(VI) in the South African FeCr industry, S. African Inst. Min. M., 110, 743–750, 2010.

Charlson, R. J.: Atmospheric visibility related to aerosol mass concentration: review, Environ. Sci. Technol., 3, 913–918, doi:10.1021/es60033a002, 1969.

Draxler, R. R. and Hess, G. D.: Description of the HYSPLIT_4 Modelling System, NOAA Technical Memorandum ERL ARL–224, 2004.

Forster, P., Ramaswamy, V., Artaxo, P., Berntsen, T., Betts, R., Fahey, D. W., Haywood, J., Lean, J., Lowe, D. C., Myhre, G., Nganga, J., Prinn, R., Raga, G., Schulz, M., and Van Dorland, R.: Changes in Atmospheric Constituents and in Radiative Forcing. In: Climate Change 2007: The Physical Science Basis. Contribution of Working Group I to the Fourth Assessment Report of the Intergovernmental Panel on Climate Change, edited by: Solomon, S., Qin, D., Manning, M., Chen, Z., Marquis, M., Averyt, K. B., Tignor, M., and Miller, H. L., Cambridge University Press, Cambridge, UK and New York, NY, USA, 136, 2007.

Friedl, M. A., McIver, D. K., Hodges, J. C. F., Zhang, X. Y., Muchoney, D., Strahler, A. H., Woodcock, C. E., Gopal, S., Schneider, A., Cooper, A., Baccini, A., Gao, F., and Schaaf, C.: Global land cover mapping from MODIS: algorithms and early results, Remote Sens. Environ., 83, 287–302, doi:10.1016/S0034-4257(02)00078-0, 2002.

Gustafsson, Ö., Krusa, M., Zencak, Z., Sheesley, R. J., Granat, L., Engström, E., Praveen, P. S., Rao, P. S. P., Leck, C., and Rodhe, H.: Brown clouds over South Asia: biomass or fossil fuel combustion?, Science, 323, 495–498, 2009.






ACPD
12, 24043–24093, 2012



Haywood, J., Francis, P., Dubovik, O., Glew, M., and Holben, B.: Comparison of aerosol size distributions, radiative properties, and optical depths determined by aircraft observations and Sun photometers during SAFARI 2000, J. Geophys. Res., 108, 8471, doi:10.1029/2002JD002250, 2003a.

Haywood, J. M., Osborne, S. R., Francis, P. N., Keil, A., Formenti, P., Andreae, M. O., and Kaye, P. H.: The mean physical and optical properties of regional haze dominated by biomass burning aerosol measured from the C-130 aircraft during SAFARI 2000, J. Geophys. Res., 108, 8473, doi:10.1029/2002JD002226, 2003b.

Hirsikko, A., Vakkari, V., Tiitta, P., Manninen, H. E., Gagné, S., Laakso, H., Kulmala, M., Mirme, A., Mirme, S., Mabaso, D., Beukes, J. P., and Laakso, L.: Characterisation of submicron particle number concentrations and formation events in the western Bushveld Igneous Complex, South Africa, Atmos. Chem. Phys., 12, 3951–3967, doi:10.5194/acp-12-3951-2012, 2012.

Hobbs, P. V., Sinha, P., Yokelson, R. J., Christian, T. J., Blake, D. R., Gao, S., Kirchstetter, T. W., Novakov, T., and Pilewskie, P.: Evolution of gases and particles from a savannah fire in South Africa, J. Geophys. Res., 108, 8485, doi:10.1029/2002JD002352, 2003.

Hoppel, W. A.: Determination of the aerosol size distribution from the mobility distribution of the charged fraction of aerosols, J. Aerosol Sci., 9, 41–54, 1978.

Hyvärinen, A.-P., Lihavainen, H., Komppula, M., Sharma, V. P., Kerminen, V.-M., Panwar, T. S., and Viisanen, Y.: Continuous measurements of optical properties of atmospheric aerosols in Mukteshwar, Northern India, J. Geophys. Res., 114, D08207, doi:10.1029/2008JD011489, 2009.

Hyvärinen, A.-P., Raatikainen, T., Komppula, M., Mielonen, T., Sundström, A.-M., Brus, D., Panwar, T. S., Hooda, R. K., Sharma, V. P., de Leeuw, G., and Lihavainen, H.: Effect of the summer monsoon on aerosols at two measurement stations in Northern India – Part 2: Physical and optical properties, Atmos. Chem. Phys., 11, 8283–8294, doi:10.5194/acp-11-8283-2011, 2011.

Jayaratne, E. R. and Verma, T. S.: The impact of biomass burning on the environmental aerosol concentration in Gaborone, Botswana, Atmos. Environ., 35, 1821–1828, 2001.

Jokinen, V. and Mäkelä, J. M.: Closed loop arrangement with critical orifice for DMA sheath/excess flow system, J. Aerosol Sci., 28, 643–648, 1997.

Kulmala, M., Asmi, A., Lappalainen, H. K., Carslaw, K. S., Pöschl, U., Baltensperger, U., Hov, Ø., Brenquier, J.-L., Pandis, S. N., Facchini, M. C., Hansson, H.-C., Wiedensohler, A.,





ACPD
12, 24043–24093, 2012



and O'Dowd, C. D.: Introduction: European Integrated Project on Aerosol Cloud Climate and Air Quality interactions (EUCAARI) – integrating aerosol research from nano to global scales, Atmos. Chem. Phys., 9, 2825–2841, doi:10.5194/acp-9-2825-2009, 2009.

Kulmala, M., Asmi, A., Lappalainen, H. K., Baltensperger, U., Brenguier, J.-L., Facchini, M. C., Hansson, H. C., Hov, Ø., O'Dowd, C. D., Pöschl, U., Wiedensohler, A., Boers, R., Boucher, O., de Leeuw, G., Denier van der Gon, H. A. C., Feichter, J., Krejci, R., Laj, P., Lihavainen, H., Lohmann, U., McFiggans, G., Mentel, T., Pilinis, C., Riipinen, I., Schulz, M., Stohl, A., Swietlicki, E., Vignati, E., Alves, C., Amann, M., Ammann, M., Arabas, S., Artaxo, P., Baars, H., Beddows, D. C. S., Bergström, R., Beukes, J. P., Bilde, M., Burkhart, J. F., Canonaco, F., Clegg, S. L., Coe, H., Crumeyrolle, S., D'Anna, B., Decesari, S., Gilardoni, S., Fischer, M., Fjaeraa, A. M., Fountoukis, C., George, C., Gomes, L., Halloran, P., Hamburger, T., Harrison, R. M., Herrmann, H., Hoffmann, T., Hoose, C., Hu, M., Hyvärinen, A., Hõrrak, U., Iinuma, Y., Iversen, T., Josipovic, M., Kanakidou, M., Kiendler-Scharr, A., Kirkevåg, A., Kiss, G., Klimont, Z., Kolmonen, P., Komppula, M., Kristjánsson, J.-E., Laakso, L., Laaksonen, A., Labonnote, L., Lanz, V. A., Lehtinen, K. E. J., Rizzo, L. V., Makkonen, R., Manninen, H. E., McMeeking, G., Merikanto, J., Minikin, A., Mirme, S., Morgan, W. T., Nemitz, E., O'Donnell, D., Panwar, T. S., Pawlowska, H., Petzold, A., Pienaar, J. J., Pio, C., Plass-Duelmer, C., Prévôt, A. S. H., Pryor, S., Reddington, C. L., Roberts, G., Rosenfeld, D., Schwarz, J., Seland, Ø., Sellegri, K., Shen, X. J., Shiraiwa, M., Siebert, H., Sierau, B., Simpson, D., Sun, J. Y., Topping, D., Tunved, P., Vaattovaara, P., Vakkari, V., Veefkind, J. P., Visschedijk, A., Vuollekoski, H., Vuolo, R., Wehner, B., Wildt, J., Woodward, S., Worsnop, D. R., van Zadelhoff, G.-J., Zardini, A. A., Zhang, K., van Zyl, P. G., Kerminen, V.-M., S Carslaw, K., and Pandis, S. N.: General overview: European Integrated project on Aerosol Cloud Climate and Air Quality interactions (EUCAARI) – integrating aerosol research from nano to global scales, Atmos. Chem. Phys., 11, 13061–13143, doi:10.5194/acp-11-13061-2011, 2011.

Laakso, L., Koponen, I. K., Mönkkönen, P., Kulmala, M., Kerminen, V.-M., Wehner, B., Wiedensohler, A., Wu, Z., and Hu, M.: Aerosol particles in the developing world; a comparison between New Delhi in India and Beijing in China, Water Air Soil Poll., 173, 5–20, 2006.

Laakso, L., Laakso, H., Aalto, P. P., Keronen, P., Petäjä, T., Nieminen, T., Pohja, T., Siivola, E., Kulmala, M., Kgabi, N., Molefe, M., Mabaso, D., Phalatse, D., Pienaar, K., and Kerminen, V.-M.: Basic characteristics of atmospheric particles, trace gases and meteorology in a relatively clean Southern African Savannah environment, Atmos. Chem. Phys., 8, 4823–4839, doi:10.5194/acp-8-4823-2008, 2008.





ACPD
12, 24043–24093, 2012



Laakso, L., Vakkari, V., Virkkula, A., Laakso, H., Backman, J., Kulmala, M., Beukes, J. P., van Zyl, P. G., Tiitta, P., Josipovic, M., Pienaar, J. J., Chiloane, K., Gilardoni, S., Vignati, E., Wiedensohler, A., Tuch, T., Birmili, W., Piketh, S., Collett, K., Fourie, G. D., Komppula, M., Lihavainen, H., de Leeuw, G., and Kerminen, V.-M.: South African EUCAARI measurements: seasonal variation of trace gases and aerosol optical properties, Atmos. Chem. Phys., 12, 1847–1864, doi:10.5194/acp-12-1847-2012, 2012.

Lourens, A. S. M., Butler, T. M., Beukes, J. P., Van Zyl, P. G., Beirle, S., Wagner, T., Heue, K.-P., Pienaar, J. J., Fourie, G. D., and Lawrence, M. G.: Re-evaluating the $NO_2$ hotspot over the South African Highveld, S. Afr. J. Sci., accepted, 2012.

Martin, S. T., Andreae, M. O., Artaxo, P., Baumgardner, D., Chen, Q., Goldstein, A. H., Guenther, A., Heald, C. L., Mayol-Bracero, O. L., McMurry, P. H., Pauliquevis, T., Pöschl, U., Prather, K. A., Roberts, G. C., Saleska, S. R., Silva-Dias, M. A., Spracklen, D. V., Swietlicki, E., and Trebs, I.: Sources and properties of Amazonian aerosol particles, Rev. Geophys., 48, RG2002, doi:10.1029/2008RG000280, 2010.

Mucina, L. and Rutherford, M. C. (Eds.): The vegetation of South Africa, Lesotho and Swaziland, South African National Biodiversity Institute, Pretoria, Republic of South Africa, 2006.

Petäjä, T., Laakso, L., Pohja, T., Siivola, E., Laakso, H., Aalto, P. P., Keronen, P., Kgabi, N. A., and Kulmala, M.: Mobile air quality monitoring trailer for developing countries, Proceedings of International Conference on Nucleation and Atmospheric Aerosols 2007, August 2007, Galway, Ireland, 2007.

Pope, C. A. and Dockery, D. W.: Health effects of fine particulate air pollution: lines that connect, J. Air Waste Manag. Assoc., 56, 709–742, 2006.

Raatikainen, T., Hyvärinen, A.-P., Hatakka, J., Panwar, T. S., Hooda, R. K., Sharma, V. P., and Lihavainen, H.: Comparison of aerosol properties from the Indian Himalayas and the Indo-Gangetic plains, Atmos. Chem. Phys. Discuss., 11, 11417–11453, doi:10.5194/acpd-11-11417-2011, 2011.

Riddle, E. E., Voss, P. B., Stohl, A., Holcomb, D., Maczka, D., Washburn, K., and Talbot, R. W.: Trajectory model validation using newly developed altitude-controlled balloons during the International Consortium for Atmospheric Research on Transport and Transformations 2004 campaign, J. Geophys. Res., 111, D23S57, doi:10.1029/2006JD007456, 2006.

Rissler, J., Vestin, A., Swietlicki, E., Fisch, G., Zhou, J., Artaxo, P., and Andreae, M. O.: Size distribution and hygroscopic properties of aerosol particles from dry-season biomass burning in Amazonia, Atmos. Chem. Phys., 6, 471–491, doi:10.5194/acp-6-471-2006, 2006.





ACPD
12, 24043–24093, 2012



Ross, K. E., Piketh, S. J., Bruintjes, R. T., Burger, R. P., Swap, R. J., and Annegarn, H. J.,: Spatial and seasonal variations in CCN distribution and the aerosol-CCN relationship over Southern Africa, J. Geophys. Res., 108, 8481, doi:10.1029/2002JD002384, 2003.

Roy, D. P., Boschetti, L., Justice, C. O., and Ju., J.: The Collection 5 MODIS Burned Area Product – Global Evaluation by Comparison with the MODIS Active Fire Product, Remote Sens. Environ., 112, 3690–3707, 2008.

Schmeissner, T., Krejci, R., Ström, J., Birmili, W., Wiedensohler, A., Hochschild, G., Gross, J., Hoffmann, P., and Calderon, S.: Analysis of number size distributions of tropical free tropospheric aerosol particles observed at Pico Espejo (4765 m a.s.l.), Venezuela, Atmos. Chem. Phys., 11, 3319–3332, doi:10.5194/acp-11-3319-2011, 2011.

Scott, G. M.: The Development of a Methodology for the Delineation of Air Quality Management Areas in South Africa, Ph.D. thesis, University of KwaZulu Natal, Durban, 2010.

Seinfeld, J. H. and Pandis, S. N.: Atmospheric Chemistry and Physics: from Air Pollution to Climate Change, 2nd ed., John Wiley and Sons, Inc., New York, 2006.

Shen, X. J., Sun, J. Y., Zhang, Y. M., Wehner, B., Nowak, A., Tuch, T., Zhang, X. C., Wang, T. T., Zhou, H. G., Zhang, X. L., Dong, F., Birmili, W., and Wiedensohler, A.: First long-term study of particle number size distributions and new particle formation events of regional aerosol in the North China Plain, Atmos. Chem. Phys., 11, 1565–1580, doi:10.5194/acp-11-1565-2011, 2011.

Sheridan, P. J., Delene, D. J., and Ogren, J. A.: Four years of continuous surface aerosol measurements from the Department of Energy's Atmospheric Radiation Measurement Program Southern Great Plains Cloud and Radiation Testbed site, J. Geophys. Res., 106, 20735–20747, 2001.

Spracklen, D. V., Carslaw, K. S., Merikanto, J., Mann, G. W., Reddington, C. L., Pickering, S., Ogren, J. A., Andrews, E., Baltensperger, U., Weingartner, E., Boy, M., Kulmala, M., Laakso, L., Lihavainen, H., Kivekäs, N., Komppula, M., Mihalopoulos, N., Kouvarakis, G., Jennings, S. G., O'Dowd, C., Birmili, W., Wiedensohler, A., Weller, R., Gras, J., Laj, P., Sellegri, K., Bonn, B., Krejci, R., Laaksonen, A., Hamed, A., Minikin, A., Harrison, R. M., Talbot, R., and Sun, J.: Explaining global surface aerosol number concentrations in terms of primary emissions and particle formation, Atmos. Chem. Phys., 10, 4775–4793, doi:10.5194/acp-10-4775-2010, 2010.

Stohl, A.: Computation, accuracy and application of trajectories – a review and bibliography, Atmos. Environ., 32, 947–966, 1998.





ACPD
12, 24043–24093, 2012



Swap, R. J., Annegarn, H. J., Suttles, J. T., King, M. D., Platnick, S., Privette, J. L., and Scholes, R. J.: Africa burning: a thematic analysis of the Southern African Regional Science Initiative (SAFARI 2000), J. Geophys. Res., 108, 8465, doi:10.1029/2003JD003747, 2003.

Tyson, P. D., Garstang, M., and Swap, R.: Large-scale recirculation of Air over Southern Africa, J. Appl. Meteorol., 35, 2218–2236, 1996.

Vakkari, V., Laakso, H., Kulmala, M., Laaksonen, A., Mabaso, D., Molefe, M., Kgabi, N., and Laakso, L.: New particle formation events in semi-clean South African savannah, Atmos. Chem. Phys., 11, 3333–3346, doi:10.5194/acp-11-3333-2011, 2011.

van Schalkwyk, M.: Notice of intention to declare the Highveld priority area in terms section 18(1) of the national environmental management air quality act, 2004 (act no. 39 of 2004), Government Gazette Republic of South Africa, 29864, 3–4, available at: http://www.info.gov.za/view/DownloadFileAction?id=73046, 2007.

Vartiainen, E., Kulmala, M., Ehn, M., Hirsikko, A., Junninen, H., Petäjä, T., Sogacheva, L., Kuokka, S., Hillamo, R., Skorokhod, A., Belikov, I., Elansky, N., and Kerminen, V.-M.: Ion and particle number concentrations and size distributions along the Trans-Siberian railroad, Boreal Environ. Res., 12, 375–396, 2007.

Venter, A. D., Vakkari, V., Beukes, J. P., van Zyl, P. G., Laakso, H., Mabaso, D., Tiitta, P., Josipovic, M., Kulmala, M., Pienaar, J. J., and Laakso, L.: An air quality assessment in the industrialized western Bushveld Igneous Complex, South Africa, S. Afr. J. Sci., accepted, 2012.

Yako, P.: Notice of intention to declare the Vaal Triangle priority area in terms section 18(1) of the national environmental management air quality act, 2004 (act no. 39 of 2004), Government Gazette Republic of South Africa, 28132, 3–4, available at: http://www.info.gov.za/view/DownloadFileAction?id=61585, 2005.





ACPD
12, 24043–24093, 2012



**Table 1.** Median and mean aerosol number concentrations for Botsalano and Marikana on different size ranges. Medians are indicated with bold font. Number concentrations, locations an short descriptions of the selected comparison measurements are also included.

| Location and time | Site | Description | Number concentration ($cm^{-3}$) | | | | Reference |
|---|---|---|---|---|---|---|---|
| 25.54° S, 25.75° E | | Diameter range (nm) | 12–840 | 12–25 | 50–840 | 100–840 | |
| 2006/7–2008/1 | Botsalano, South Africa | Semi-clean savannah | **1856** | **152** | **1278** | **698** | This study |
| | | | 3825 | 824 | 1914 | 875 | |
| 25.70° S, 27.48° E | | Diameter range (nm) | 12–840 | 12–25 | 50–840 | 100–840 | |
| 2008/2–2010/5 | Marikana, South Africa | Polluted savannah | **7805** | **1725** | **3843** | **1634** | This study |
| | | | 14 048 | 4237 | 5737 | 2194 | |
| 29.43° N, 79.62° E | | Diameter range (nm) | 3–800 | 3–25 | 25–75 | 75–800 | |
| 2006–2009 | Mukteswhar, India | Rural cropland | 3828[a] | 176[a] | 1277[a] | 2373[a] | Hyvärinen et al. (2011) |
| 28.43° N, 77.15° E | | Diameter range (nm) | 3–800 | 3–25 | 25–75 | 75–800 | |
| 2008–2009 | Gual Pahari, India | Semi-urban megacity | 25860[b] | 1950[b] | 6904[b] | 5150[a] | Hyvärinen et al. (2011) |
| | | | | | | 16966[b] | |
| 40.65° N, 117.12° E | | Diameter range (nm) | 3–10 000 | 3–25 | 25–100 | 100–10 000 | |
| 2008/3–2009/8 | Shangdianzi, China | Semi-clean crop/grassland | 11 510 | 3610 | 4430 | 3470 | Shen et al. (2011) |
| 36.61° N, 97.49° W | | Diameter range (nm) | 10–3000 | | | 100–10 000 | |
| 1996/7–2000/6 | Southern Great Plains, US | Semi-clean crop/grassland | 4500 | | | 430 | Sheridan et al. (2001) |
| 46.97° N, 19.55° E | | Diameter range (nm) | | 30–50 | 50–500 | 100–500 | |
| 2008–2009 | K-Puszta, Hungary | Semi-clean crop/grassland | | **697** | **3120** | **1660** | Asmi et al. (2011) |
| | | | | 979 | 3669 | 1952 | |
| 45.82° N, 8.63° E | | Diameter range (nm) | | 30–50 | 50–500 | 100–500 | |
| 2008–2009 | Ispra, Italy | Polluted industrial | | **1341** | **4448** | **2129** | Asmi et al. (2011) |
| | | | | 1617 | 5571 | 2888 | |
| 26.23° S, 29.42° E | | Diameter range (nm) | 10–10 000 | | | | |
| 2009/2–2011/1 | Elandsfontein, South Africa | Semi-polluted crop/grassland | 6310 | | | | Laakso et al. (2012) |
| 24.65° S, 25.90° E | | Diameter range (nm) | | | | 100–5000 | |
| 1999/9–2000/10 | Gaborone, Botswana | Urban | | | | 1000 | Jayaratne and Verma (2001) |
| 10.76° S, 62.36° W | | Diameter range (nm) | 3–850 | | 30–850 | | |
| 9/2005–11/2005 | Rondonia, Brazil | Clean crop/grassland | 11 440[c] | | 10 440[c] | | Rissler et al. (2006) |
| | | | 2070[d] | | 1280[d] | | |

[a] Calculated as a mean of pre-monsoon, monsoon and post-monsoon values in the original paper (Hyvärinen et al., 2011). [b] Only post-monsoon 2009 (October to November). [c] End of dry season (11 September–8 October 2005). [d] Beginning of wet season (31 October–14 November 2005).





ACPD
12, 24043–24093, 2012



**Table 2.** Size distribution parameters for Botsalano and Marikana. Negative mean relative error (MRE) values indicate overestimation by the modal fits.

| | mode 1 ($N$ ($cm^{-3}$), $\mu$ (nm), $\sigma$) | mode 2 ($N$ ($cm^{-3}$), $\mu$ (nm), $\sigma$) | mode 3 ($N$ ($cm^{-3}$), $\mu$ (nm), $\sigma$) | MRE (%) (all, < 300 nm, > 300 nm) |
|---|---|---|---|---|
| Botsalano | | | | |
| Median | | 1501, 61.2, 2.07 | 370, 161.0, 1.48 | −5, 3, −30 |
| Mean | 1474, 18.1, 2.02 | 2474, 60.2, 2.00 | 288, 185.0, 1.39 | 2, 0.5, 8 |
| Marikana | | | | |
| Median | 2040, 13.7, 1.80 | 6438, 54.8, 2.12 | 274, 195.6, 1.37 | 1, 0.08, 4 |
| Mean | 7204, 12.9, 1.87 | 9992, 53.5, 2.07 | 214, 205.6, 1.30 | 6, 0.3, 25 |





ACPD
12, 24043–24093, 2012



**Table 3.** Size distribution parameters for median distributions at 06:00, 12:00, 18:00 and 24:00 LT for Botsalano and Marikana.

| | Fractional concentrations | | | Modal fitting parameters | | | |
|---|---|---|---|---|---|---|---|
| | $N12$ ($cm^{-3}$) | $N50$ ($cm^{-3}$) | $N100$ ($cm^{-3}$) | mode 1 ($N$ ($cm^{-3}$), $\mu$ (nm), $\sigma$) | mode 2 ($N$ ($cm^{-3}$), $\mu$ (nm), $\sigma$) | mode 3 ($N$ ($cm^{-3}$), $\mu$ (nm), $\sigma$) | MRE (%) (all, < 300 nm, > 300 nm) |
| Botsalano | | | | | | | |
| 06:00 | 1540 | 1150 | 616 | 1055, 16.6, 1.65 | 1332, 71.6, 1.94 | 212, 182, 1.39 | 3, 2, 6 |
| 12:00 | 2366 | 1333 | 766 | | 1295, 82.7, 1.83 | 278, 175, 1.40 | 5, 0.1, 22 |
| 18:00 | 1997 | 1231 | 701 | | 1144, 39.0, 1.75 | 877, 136, 1.60 | −0.7, 3, −11 |
| 24:00 | 1881 | 1307 | 684 | | 1585, 63.1, 1.97 | 305, 173, 1.41 | 4, 0.6, 14 |
| Marikana | | | | | | | |
| 06:00 | 7850 | 3740 | 1637 | 4413, 15.4, 1.98 | 4709, 69.3, 1.90 | 274, 214, 1.39 | 8, −0.01, 34 |
| 12:00 | 11545 | 2974 | 1395 | 11433, 20.9, 1.84 | 1769, 107, 1.50 | 329, 225, 1.30 | 17, −0.1, 73 |
| 18:00 | 11 114 | 5026 | 1815 | 1412, 12.8, 1.52 | 9923, 45.1, 1.97 | 587, 190, 1.36 | 16, 0.02, 65 |
| 24:00 | 7460 | 4394 | 1821 | 1479, 15.1, 1.62 | 6055, 64.2, 1.85 | 371, 206, 1.36 | 14, 0.02, 57 |





ACPD
12, 24043–24093, 2012



**Table 4.** Seasonal median distribution parameters for Botsalano and Marikana. Summer is December to February, autumn is March to May, winter is June to August and spring is September to November.

| | Fractional concentrations | | | Modal fitting parameters | | | |
|---|---|---|---|---|---|---|---|
| | $N12$ ($cm^{-3}$) | $N50$ ($cm^{-3}$) | $N100$ ($cm^{-3}$) | mode 1 ($N$ ($cm^{-3}$), $\mu$ (nm), $\sigma$) | mode 2 ($N$ ($cm^{-3}$), $\mu$ (nm), $\sigma$) | mode 3 ($N$ ($cm^{-3}$), $\mu$ (nm), $\sigma$) | MRE (%) (all, < 300 nm, > 300 nm) |
| Botsalano | | | | | | | |
| Summer | 1778 | 1235 | 623 | 666, 31.3, 1.61 | 1473, 62.4, 1.91 | 299, 171, 1.45 | 8, 6, 17 |
| Autumn | 1852 | 1202 | 653 | | 1544, 57.1, 2.13 | 334, 163, 1.44 | −10, 2, −50 |
| Winter | 2145 | 1409 | 750 | | 1331, 92.8, 1.77 | 151, 177, 1.36 | 8, 3, 22 |
| Spring | 1769 | 1301 | 775 | | 1114, 56.5, 1.97 | 665, 56, 1.57 | 1, 3, −5 |
| Marikana | | | | | | | |
| Summer | 6619 | 3022 | 1245 | 888, 13.2, 1.41 | 6134, 45.4, 2.25 | 233, 198, 1.36 | −2, 0.02, −10 |
| Autumn | 8330 | 4003 | 1646 | 2597, 14.7, 1.81 | 6510, 56.5, 2.05 | 242, 200, 1.34 | 4, 0.07, 16 |
| Winter | 10 070 | 5834 | 2544 | 1558, 15.3, 1.74 | 8974, 63.7, 2.07 | 148, 184, 1.34 | −4, 0.1, −18 |
| Spring | 6788 | 3112 | 1436 | 5888, 24.8, 2.66 | 1630, 66.7, 1.84 | 604, 180, 1.48 | 0.6, 0.2, 2 |





ACPD
12, 24043–24093, 2012



**Table 5.** Criteria for source region characterisation and the number of size distribution measurements obtained for each source region. Also average number of observations per each 10 min average in the average diurnal variation in Fig. 13 is included.

| | Re-circulation | Industrial hub | Kalahari | Karoo |
|---|---|---|---|---|
| Minimum time over source region | 72 h | 24 h | 48 h | 48 h |
| Maximum time over other areas | 0 h on any other | 24 h over re-circulation, 12 h over clean sector | 10 h over re-circulation, 24 h total over Karoo and recirculation | 0 h over any other |
| Number of size spectra | 13 000 | 1200 | 1100 | 2000 |
| Size spectra/ 10 min average | 90 | 8 | 7 | 14 |





ACPD
12, 24043–24093, 2012



**Table 6.** Size distribution parameters for the four source regions defined for Botsalano.

| | Fractional concentrations | | | Modal fitting parameters | | | |
|---|---|---|---|---|---|---|---|
| | $N12$ ($cm^{-3}$) | $N50$ ($cm^{-3}$) | $N100$ ($cm^{-3}$) | mode 1 ($N$ ($cm^{-3}$), $\mu$ (nm), $\sigma$) | mode 2 ($N$ ($cm^{-3}$), $\mu$ (nm), $\sigma$) | mode 3 ($N$ ($cm^{-3}$), $\mu$ (nm), $\sigma$) | RME (%) (all, < 300 nm, > 300 nm) |
| Re-circulation | 2027 | 1592 | 914 | 38, 17.0, 1.49 | 1603, 77.1, 1.91 | 394, 165, 1.43 | −3, −0.5, −9 |
| Industrial hub | 2361 | 1675 | 878 | | 2150, 70.1, 2.02 | 226, 202, 1.28 | −20, −0.7, −79 |
| Kalahari | 939 | 676 | 431 | 59, 15.4, 1.50 | 522, 56.1, 1.92 | 377, 165, 1.51 | 3, −0.2, 13 |
| Karoo | 1645 | 641 | 245 | 185, 21.9, 1.29 | 1566, 40.7, 2.38 | | −19, 1, −79 |





ACPD
12, 24043–24093, 2012



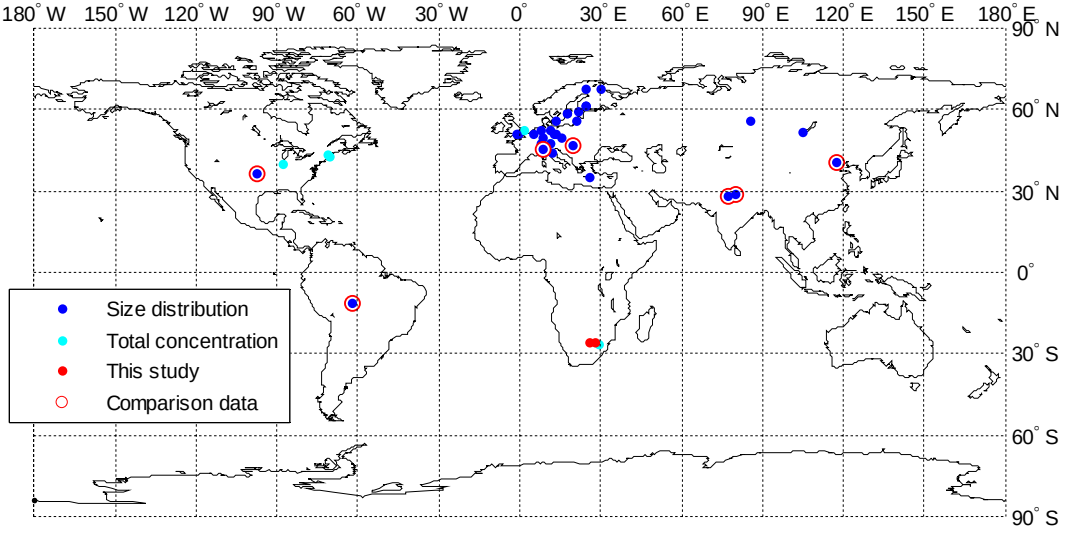


**Fig. 1.** Long-term observations of aerosol particle number size distribution or total concentration extending below 100 nm in the continental boundary layer excluding urban environments. The observations from the locations indicated with red circles are compared with the results of this study. Note that the South American comparison site had only two months of measurements.





ACPD
12, 24043–24093, 2012



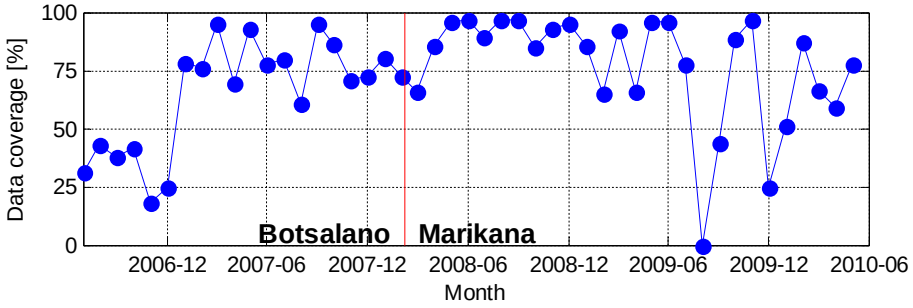


**Fig. 2.** DMPS data coverage.





ACPD
12, 24043–24093, 2012



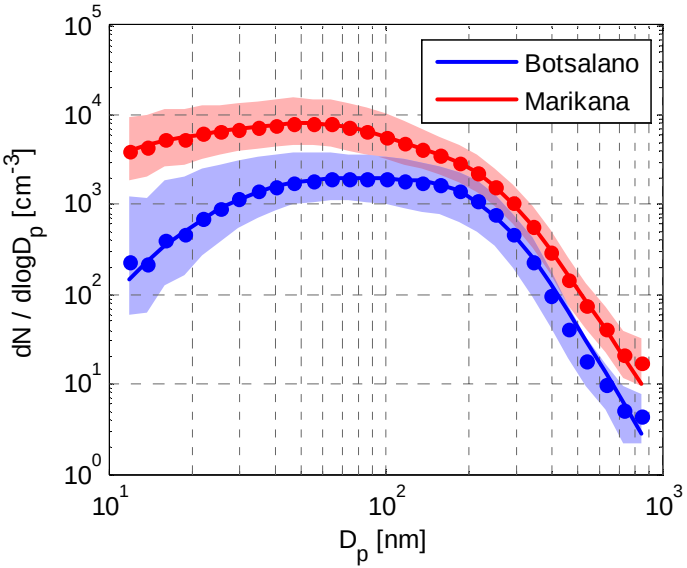


**Fig. 3.** Median distributions for Botsalano and Marikana. The dots indicate the median measured distribution and the lines show the fitted log-normal distribution from Table 2. Shaded areas indicate the upper and lower quartiles.





ACPD
12, 24043–24093, 2012



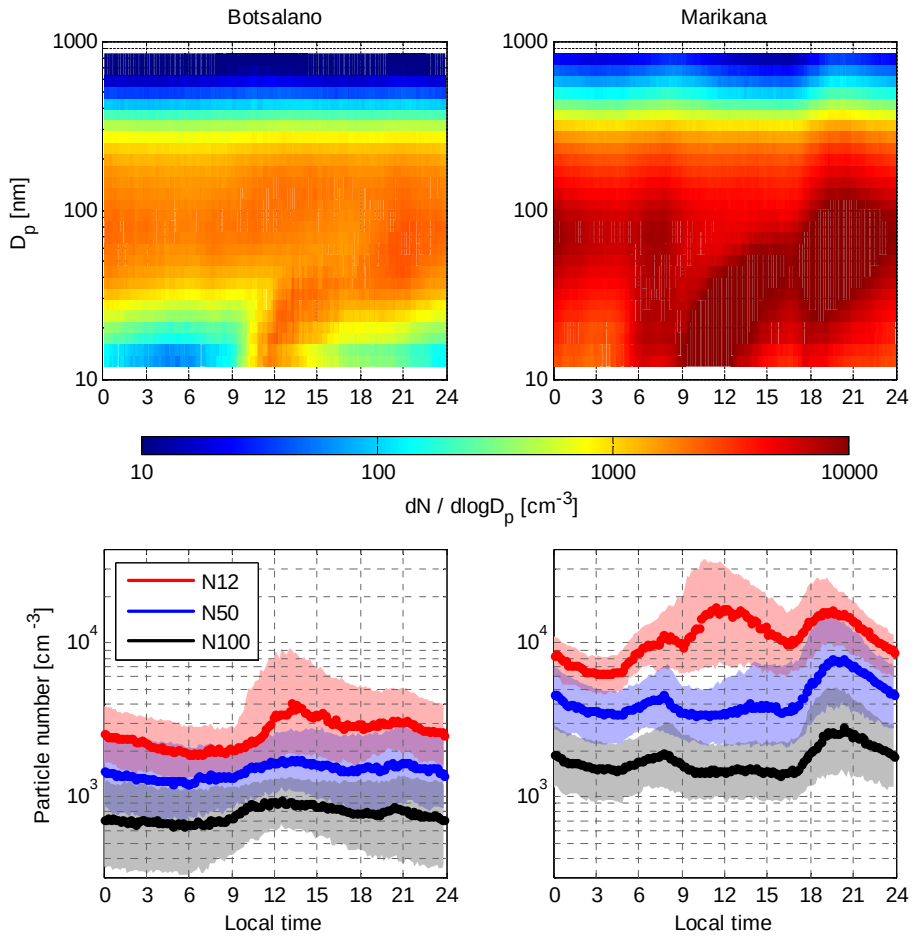


**Fig. 4.** Median diurnal variation of the aerosol particle size distribution for Botsalano and Marikana. In the lower panels the upper and lower quartiles are indicated by the shaded areas.





ACPD
12, 24043–24093, 2012



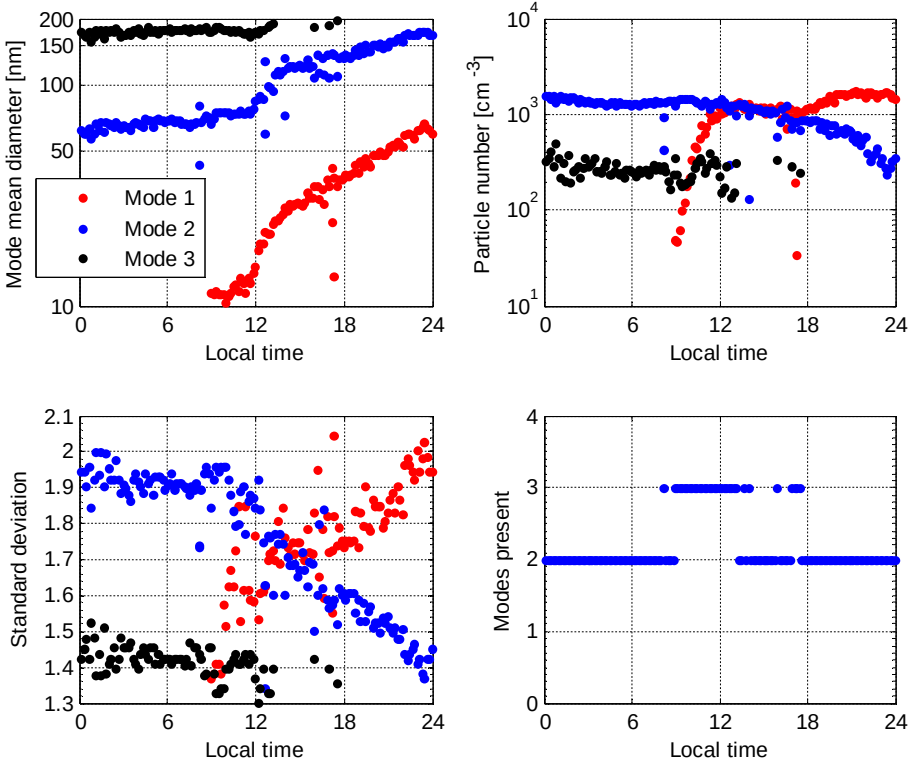


**Fig. 5.** Modal fit parameters for Botsalano median diurnal behaviour.





ACPD
12, 24043–24093, 2012



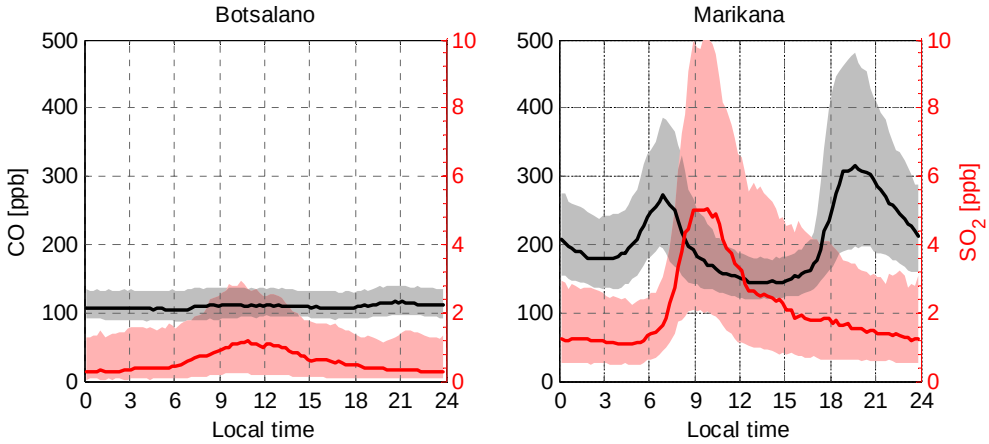


**Fig. 6.** Median $SO_2$ and CO diurnal variations for Botsalano and Marikana. Shaded areas indicate the upper and lower quartiles.





ACPD
12, 24043–24093, 2012



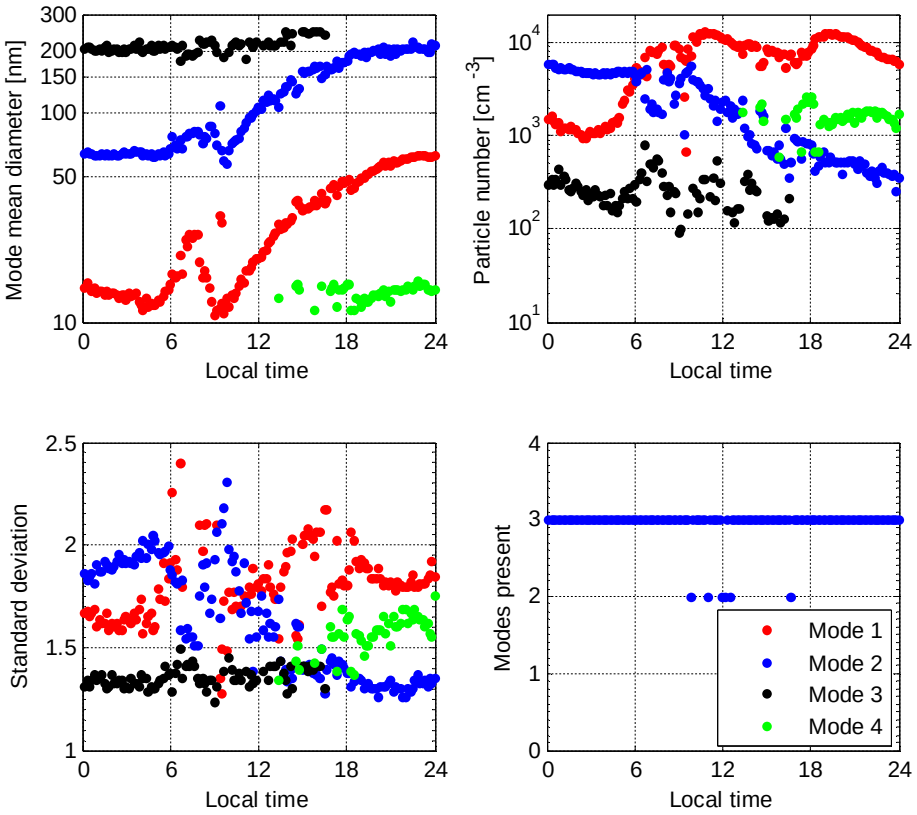


**Fig. 7.** Diurnal behaviour of the modal fitting parameters for Marikana.





ACPD
12, 24043–24093, 2012



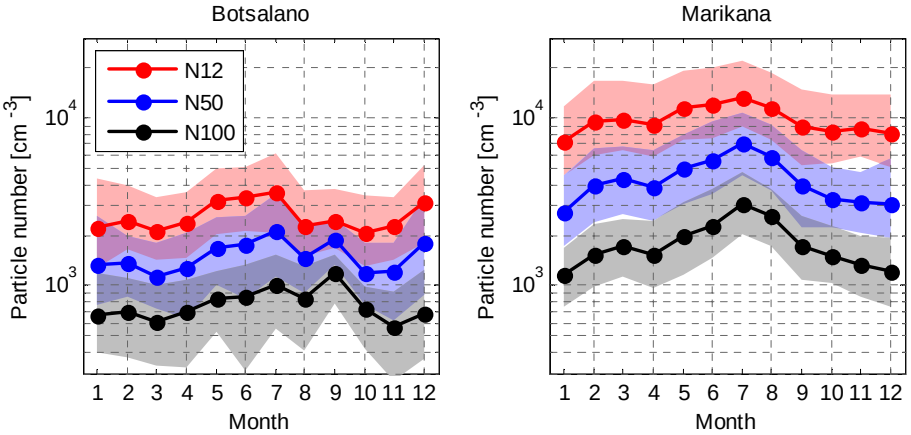


**Fig. 8.** Monthly median concentrations of *N*12, *N*50 and *N*100 for Botsalano and Marikana. Shaded areas indicate the upper and lower quartiles.





ACPD
12, 24043–24093, 2012



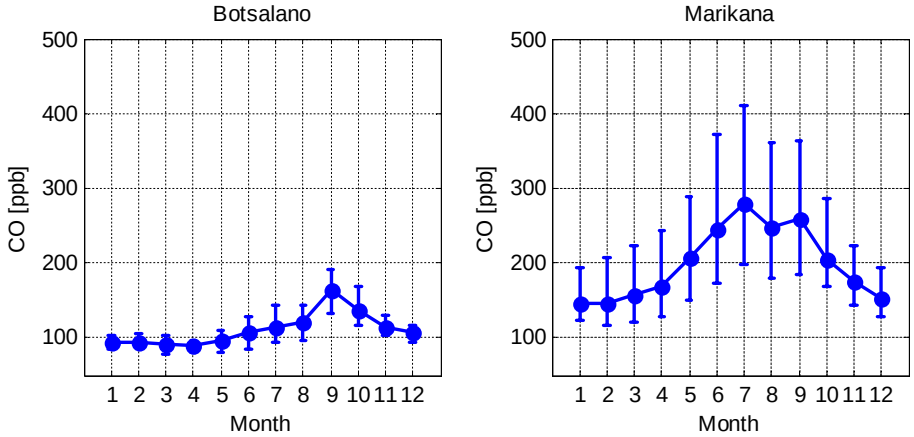


**Fig. 9.** Monthly median concentrations of CO for Botsalano and Marikana. Error bars indicate the upper and lower quartiles.





ACPD
12, 24043–24093, 2012



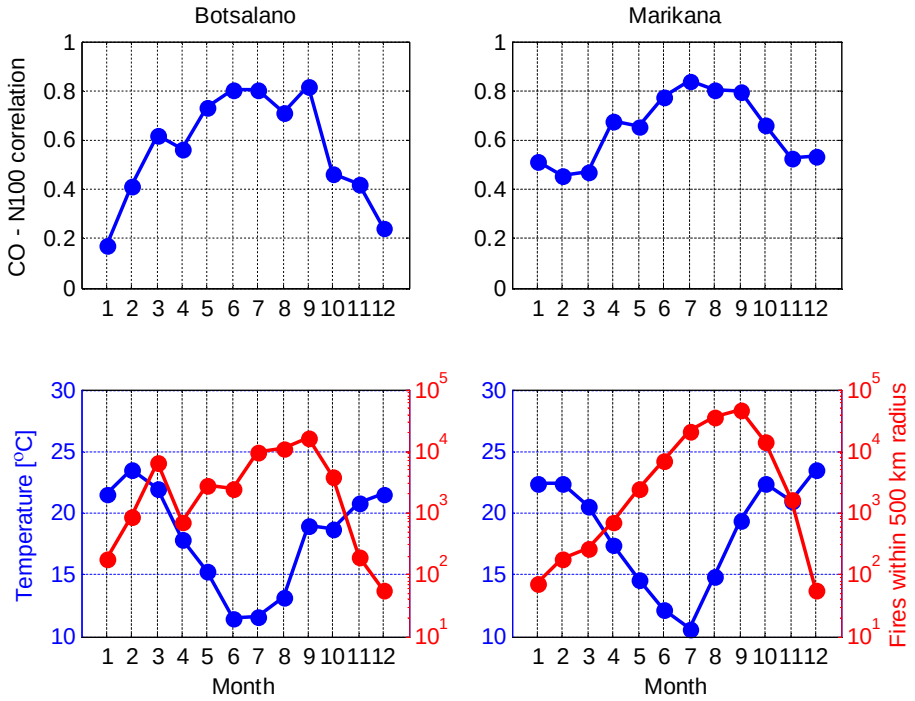


**Fig. 10.** Monthly correlation coefficient for CO and *N*100, median temperature and number of MODIS burned area fire observations within 500 km radius of measurement location for Botsalano and Marikana.





ACPD
12, 24043–24093, 2012

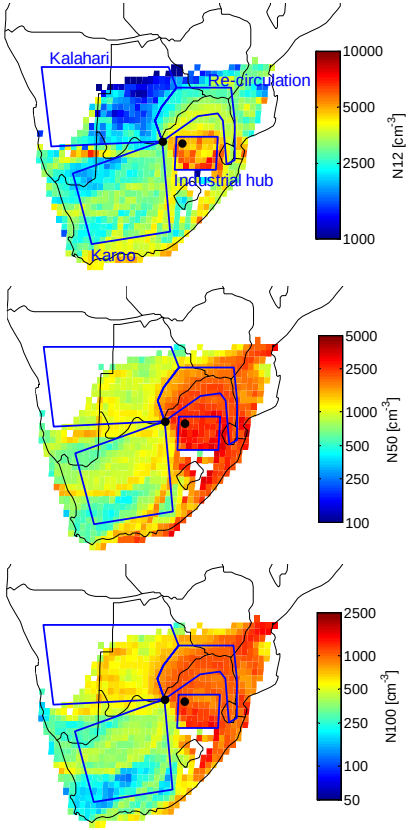


**Fig. 11.** Mean *N*12, *N*50 and *N*100 for the four defined source regions at Botsalano. Black dots indicate Botsalano on the left and the later measurement location, Marikana, on the right.





ACPD
12, 24043–24093, 2012



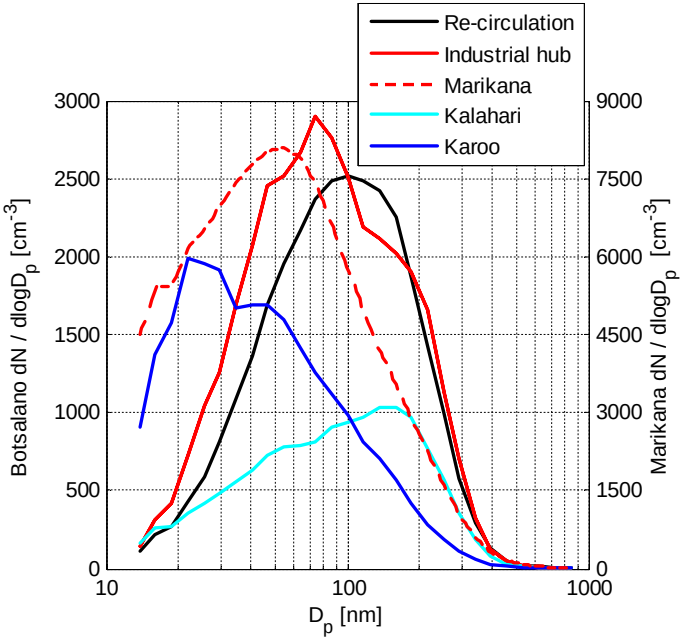


**Fig. 12.** Median size distributions for the four source regions defined for Botsalano (left axis) and the Marikana median size distribution (right axis). Modal fitting parameters are given in Table 6 for the source regions.





ACPD
12, 24043–24093, 2012



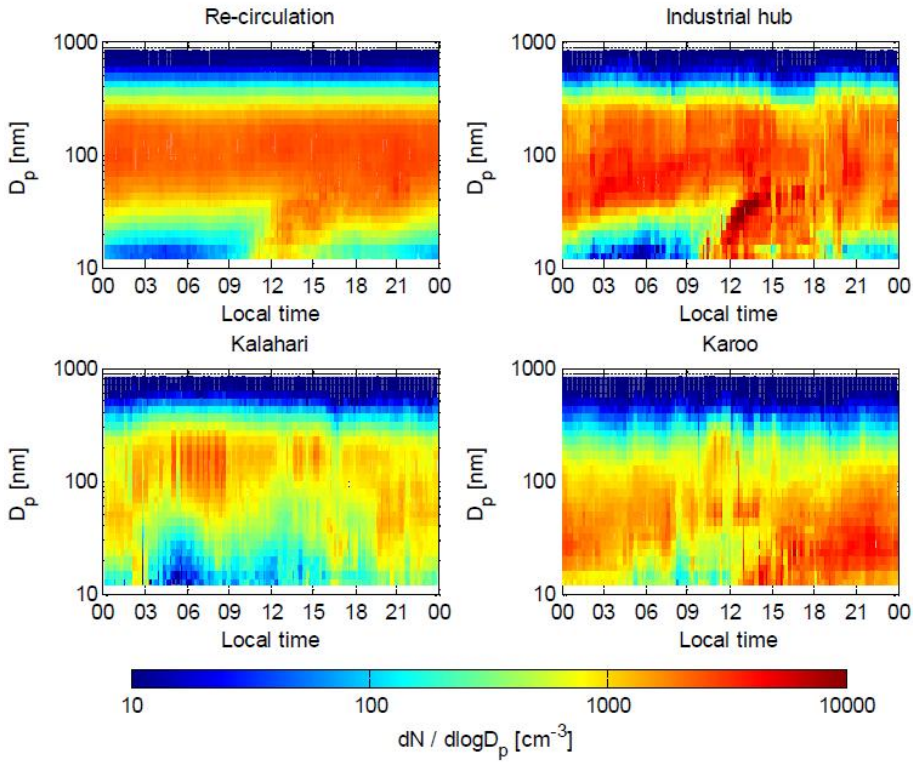


**Fig. 13.** Median diurnal variation of the size distribution for the four source regions derived for Botsalano.





ACPD
12, 24043–24093, 2012



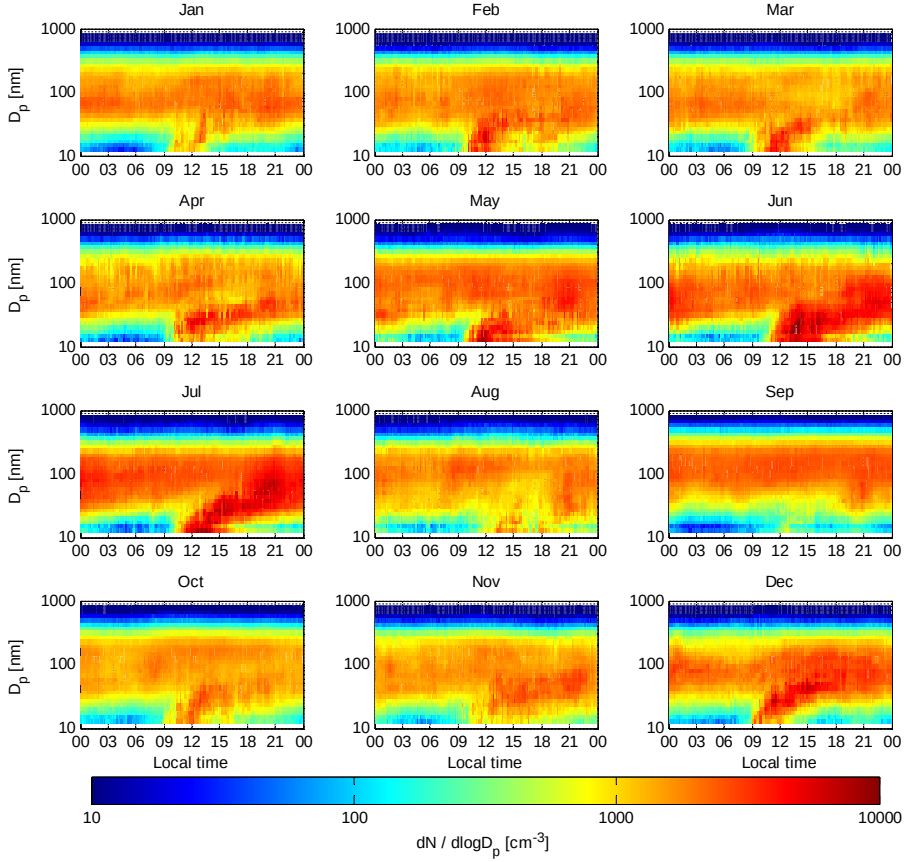


**Fig. A1.** Botsalano monthly median diurnal variation.





ACPD
12, 24043–24093, 2012

Long-term observations of aerosol size distributions

V. Vakkari et al.



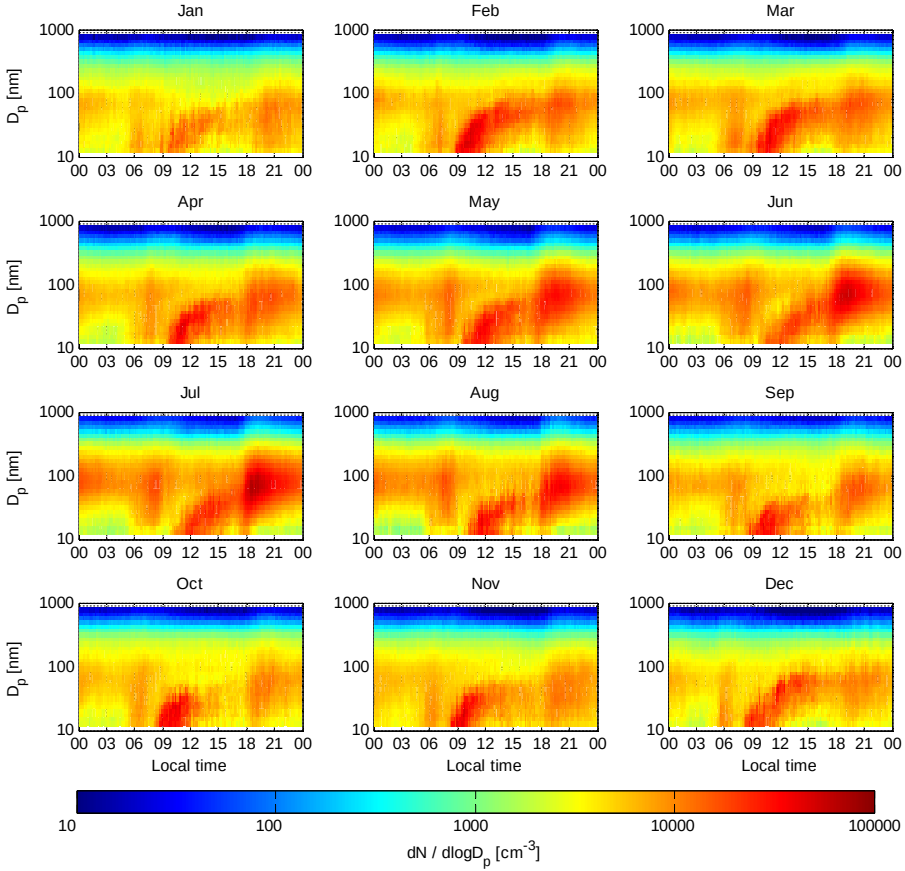


**Fig. A2.** Marikana monthly median diurnal variation. Note that the upper limit of the colour axis is increased from 10 000 $cm^{-3}$ in Fig. A1 to 100 000 $cm^{-3}$.





ACPD
12, 24043–24093, 2012